Title: Identification and analysis of sugar transporters capable of co-transporting glucose and xylose simultaneously

Nurzhan Kuanyshev[a,b], Anshu Deewan[a,b,c], Sujit Sadashiv Jagtap[a,c], Jingjing Liu[a,b], Balaji Selvam[c], Li-Qing Chen[a,e], Diwakar Shukla[c,e,f,g*], Christopher V. Rao[a,b,c*] and Yong-Su Jin[a,b,d*]

[a]DOE Center for Advanced Bioenergy and Bioproducts Innovation University of Illinois at Urbana-Champaign, Urbana, IL 61801, USA, [b]Carl R. Woese Institute for Genomic Biology, University of Illinois at Urbana-Champaign, Urbana, IL 61801, USA, [c]Department of Chemical and Biomolecular Engineering, University of Illinois at Urbana-Champaign, Urbana, IL 61801, USA, [d]Department of Food Science and Human Nutrition, University of Illinois at Urbana-Champaign, Urbana, IL 61801, USA, [e]Department of Plant Biology, University of Illinois at Urbana-Champaign, Urbana, IL 61801, USA, [f]NIH Center for Macromolecular Modeling and Bioinformatics, University of Illinois at Urbana-Champaign, Urbana, IL 61801, USA, [g]Beckman Institute for Advanced Science and Technology, University of Illinois at Urbana-Champaign, Urbana, IL 61801, USA.

Corresponding authors: *Diwakar Shukla**,** *Christopher V Rao and *Yong-Su Jin, Carl R., 211 Roger Adams Laboratory, 600 S Mathews Ave, Urbana, IL 61801, cvrao@illinois.edu, 203 Roger Adams Laboratory, 600 S Mathews Ave, Urbana, IL 61801 diwakar@illinois.edu, and Carl R. Woese Institute for Genomic Biology, 1206 W Gregory Dr, Urbana, IL 61801, ysjin@illinois.edu

Abstract

Simultaneous co-fermentation of glucose and xylose is a key desired trait of engineered *Saccharomyces cerevisiae* for efficient and rapid production of biofuels and chemicals. However, glucose strongly inhibits xylose transport by endogenous hexose transporters of *S. cerevisiae*. We identified structurally distant sugar transporters (*Lipomyces starkeyi* LST1_205437 and *Arabidopsis thaliana At*SWEET7) capable of co-transporting glucose and xylose from previously unexplored oleaginous yeasts and plants. Kinetic analysis showed that LST1_205437 had lenient glucose inhibition on xylose transport and *At*SWEET7 transported glucose and xylose simultaneously with no inhibition. Modelling studies of LST1_205437 revealed that Ala335 residue at sugar binding site can accommodates both glucose and xylose. Docking studies with *At*SWEET7 revealed that Trp59, Trp183, Asn145 and Asn179 residues stabilized the sugars, allowing both xylose and glucose to be co-transported. In addition, we altered sugar preference of LST1_205437 by single amino acid mutation at Asn365. Our findings provide a new mechanistic insight on glucose and xylose transport mechanism of sugar transporters and the identified sugar transporters can be employed to develop engineered yeast strains for producing cellulosic biofuels and chemicals.

Keywords: sugar membrane transporter, co-fermentation, substrate specificity, rational evolution

1. Introduction

Glucose and xylose are the two most abundant sugars in lignocellulosic biomass (Carroll and Somerville, 2009). The development of efficient and economical processes for the conversion of lignocellulosic biomass into various biofuels, chemicals and bioproducts requires microorganisms capable of utilizing both sugars if possible simultaneously (Kim et al., 2012). Xylose metabolism, however, is not native to *Saccharomyces cerevisiae,* which has been used for the production of corn and sugarcane ethanol. A number of studies have demonstrated that *S. cerevisiae* can be engineered to efficiently utilize xylose (Brat et al., 2009; Jeffries and Jin, 2004; Jin et al., 2003; Kim et al., 2013; Kotter et al., 1990; Kuyper et al., 2003; Kwak and Jin, 2017; Zhou et al., 2012). However, xylose transport in these engineered strains is subject to glucose repression, which leads to sequential utilization of glucose and xylose rather than simultaneous co-utilization. Glucose repression in a xylose-fermenting engineered *S. cerevisiae* is initiated from glucose inhibition on xylose uptake by endogenous sugar transporters (Gardonyi et al., 2003; Hamacher et al., 2002; Parachin et al., 2011; Sedlak and Ho, 2004).

S. cerevisiae has at least 18 hexose transporters. However, dedicated xylose transporters in *S. cerevisiae* has not been reported. Xylose transport in *S. cerevisiae* is facilitated by actively expressed hexose transporters *(HXT1-7 and GAL2) as HXT8-HXT17* are either inactive (not transcribed) or cryptic (Hamacher et al., 2002; Ozcan and Johnston, 1999; Sedlak and Ho, 2004). Although these hexose transporters can facilitate efficient xylose utilization when it is the sole sugar, the presence of glucose completely inhibits xylose uptake due to the higher affinity of the sugar transporters toward glucose

(Subtil and Boles, 2012). As such, glucose inhibition of xylose transport has been considered as a bottleneck preventing simultaneous co-fermentation of glucose and xylose. Several attempts have been made to bypass glucose inhibition in mixed-sugar fermentations. Ha *et al.* developed an engineered yeast strain capable of co-fermenting cellobiose, a dimer of glucose, and xylose, thus avoiding inhibition of xylose transport by glucose (Ha et al., 2011). However, this strategy does not allow co-fermentation of monomeric sugars present in cellulosic hydrolysates generated by matured pretreatment and enzymatic hydrolysis processes (Cheng et al., 2019b; Shirkavand et al., 2016). Therefore, many studies have focused on identifying xylose specific transporters from xylose-fermenting yeast species, such as *Pichia stipitis* and *Candida intermedia* (Leandro et al., 2009; Young et al., 2011). Although heterologous expression of the identified xylose transporters in a *S. cerevisiae* lacking hexose sugar transporters conferred growth on xylose, glucose inhibition on xylose transport was still observed (Leandro et al., 2009; Young et al., 2011). In addition to bioprospecting, rational and directed-evolution approaches have led to the development of xylose transporters not inhibited by glucose (Farwick et al., 2014; Li et al., 2016; Reider Apel et al., 2016; Shin et al., 2015; Young et al., 2014). Using rational mutagenesis, Young *et al.* reported a conserved amino-acid motif responsible for monosaccharide selectivity in sugar transporters conferring growth on xylose. Further, mutation of the conserved monosaccharide recognition motifs led to a designed transporter for xylose transport. However, the transporter could not transport glucose and xylose simultaneously, leaving the co-fermentation problem open (Young et al., 2014). Farwick *et al.* employed adaptive laboratory evolution of an individual sugar transporter, using a xylose-utilizing strain of *S. cerevisiae* lacking all hexose transporters

and with disrupted glycolysis, to identify evolved hexose transporters insensitive to glucose repression. The authors discovered two amino-acid residues (Asn376/370 and Thr219/213) of Gal2 and Hxt7 that are essential for co-transport of glucose and xylose. However, modifying these two residues resulted in reduced rates of glucose and xylose transport (Farwick et al., 2014). Using similar approach Shin *et al.,* identified Asn366 residue mutation (same as in *Sc*Gal2/Hxt7 Asn376/370) in Hxt11 that enabled simultaneous glucose and xylose co-fermentation (Shin et al., 2015).

While the rational design approach led to promising results, we aimed to expand bioprospecting in the search of native glucose and xylose co-transporters. Oleaginous yeasts, such as *Rhodosporidium toruloides* and *Lipomyces starkeyi* are receiving more attention as an alternative cell factory for lipid and acetyl-CoA based products given their ability to naturally consume most of the sugars including hemicellulose derived glucose and xylose (Adrio, 2017; Zhang et al., 2016). Recently, genome sequence of *R. toruloides* and *L. starkeyi* have been reconstructed and annotated, allowing search for putative xylose transporters (Coradetti et al., 2018; Riley et al., 2016). According to our xylose transporter search criteria based on conserved motif G[G/F]XXXG (Young et al., 2014) and Thr213 and Asn370 residues (Farwick et al., 2014), both species contained 8 putative xylose transporters.

In contrast to yeast transporters, the mechanism of xylose transport by SWEETs has not been studied so far. SWEETs are newly discovered family of transporters with distinct 7 transmembrane (TM) structure that plays a key role in plant development and sugar translocation within the plant phloem (Jeena et al., 2019). SWEETs are comprised by 7 TM domains, where the N-terminal three helixes shares sequence similarity to C-

terminal three helixes, connected by non-conserved fourth domain (Chen et al., 2010; Han et al., 2017; Tao et al., 2015; Xuan et al., 2013). Previous studies on *Arabidopsis thaliana* SWEETs demonstrated functional expression of the transporters in yeast, conferring growth on glucose (Chen et al., 2010; Selvam et al., 2019; Tao et al., 2015). Recently, Podolsky *et al.,* identified novel fungal SWEET from anaerobic fungi (Neocallimastigomycota) which demonstrated co-consumption of glucose and xylose in *S. cerevisiae* (Podolsky et al., 2021).

In this study we aimed to investigate an ability of putative xylose transporters from *R. toruloides* IFO0880 and *L. starkeyi* NRRL Y-11557 and SWEET transporters from *A. thaliana* to co-ferment glucose and xylose, a desired trait for producing cellulosic biofuels by engineered *S. cerevisiae*. In the first part of the study, we expressed selected transporters in engineered *S. cerevisiae* optimized for efficient xylose fermentation lacking major hexose transporters to screen and characterize transporters that capable to co-ferment both sugars (Xu, 2015). We identified that *L. starkeyi* LST1_205437 and *A. thaliana* SWEET7 have an ability to co-ferment glucose and xylose simultaneously. To understand kinetic background behind simultaneous glucose and xylose co-fermentation, we performed kinetic study using ^{14}C labeled sugars. Kinetics studies revealed that both transporters transports xylose in the presence of glucose. Cryo-EM or/and X ray crystallography of the selected transporters have not been resolved. Hence, to explain molecular basis of this unique trait observed in the selected transporters, we employed *in silico* molecular modelling and dynamics simulation (MD). Using crystal structure of OsSWEET2b and XylE transporters as a homology template, we performed molecular simulation of glucose and xylose transport in LST1_205437 and *A. thaliana* SWEET7.

The study demonstrated that bioprospecting approach still can be a versatile tool to identify novel transporters with unorthodox protein motifs and residues for glucose and xylose cotransport. By combining kinetics and molecular simulation study, we were able to get insights into a molecular basis and responsible amino acid residues enabling co-transport of glucose and xylose in LST1_205437 and *At*SWEET7 (Fig 1).

2. Materials and Methods

2.1 Medium and cell growth conditions

Under non-selective conditions, all strains were grown YPD agar plates (2 % w/v agar, 1 % w/v yeast extract, 2 % peptone and 2 % glucose). A single colony from YPD agar plate was inoculated into 2 mL YPD liquid medium to obtain seed cultures. For growth study, the seed cultures were then used to inoculate 25 mL of YPD and YPX medium (10 g/L yeast extract, 20 g/L peptone, and 20 g/L xylose or glucose) in a 125 mL shake flask with a starting OD600 of 1. The cells were then grown at 30 °C and 250 rpm.

For flask fermentation, a single colony was inoculated to 5 or 25 mL YPE (1 % w/v yeast extract, 2 % peptone, 5 % ethanol) supplemented with 200 μg/ml of geneticin to obtain seed cultures. Subsequently, seed cultures were inoculated to 25 mL of YPD,YPX and YPDX medium (10 g/L yeast extract, 20 g/L peptone, and 20 g/L xylose or/and glucose) in a 125 mL shake flask with a starting OD600 of 1, 5 or 10 for flask fermentation. Flask fermentations were maintained at 30 °C and 250 rpm. $CaCO_3$ at 50g/L were added for high sugar fermentations in YPDX medium (10 g/L yeast extract, 20 g/L peptone, 70g/L glucose and 40g/L xylose).

A previously constructed xylose fermenting *S .cerevisiae* yeast (SR8) with *HXT1-7*Δ*, GAL2*Δ deletions was used for transporter screening and characterization (SR8D8) (Xu, 2015) (Kim et al., 2013). SR8D8 was grown in YPE medium (10 g/L yeast extract, 20 g/L peptone, and 5 g/L ethanol). The codon optimized sugar transporter genes from *L. starkeyi*, *R. toruloides* and *A. thaliana* were expressed in SR8D8 using G418 resistance dominant marker harboring plasmid for glucose and/or xylose transport characterization. SR8D8 strains transformed with plasmid containing *KanMX* marker conferring resistance to G418 (geneticin) were propagated on YPE supplemented with 200 µg/ml of geneticin. For growth and flask fermentation experiments all media was supplemented with 200 µg/ml of geneticin for plasmid maintenance. Biomass was calculated from the OD600 measured using a Biomate 5 UV-visible spectrophotometer (Fisher, NY, USA). All growth rates were measured using a Bioscreen C plate reader system (Growth Curves USA, Piscataway, NJ, USA). A 2 µL inoculum of fully-grown culture was added into 200 µL YP containing 200 µg/ml Geneticin with varying concentrations of different sugars. A wide band filter (420–580 nm) was used to measure optical density. Bioscreen C values represent mean value from three biological replicates. In all cases, the Bioscreen C was set to maintain a temperature of 30 °C and high aeration through high continuous shaking.

2.2 Plasmid construction and transformation

All transporters were cloned into p42K-GPD1p-CYC1t plasmid harboring 2µ replication origin and *KanMX* marker conferring resistance to G418 (geneticin) antibiotic. For *At*SWEET transporters p42K-GPD1p-CYC1t plasmid were linearized with BamHI and XhoI enzymes. *AtSWEET*s were PCR amplified and digested with BamHI and XhoI.

184 Linear p42K-GPD1p-CYC1t and AtSWEETs were ligated with T4 ligase according to
185 manufacturer's protocol. For *R. toruloides* and *L. starkeyi* transporters p42K-GPD1p-
186 CYC1t plasmid were linearized with BamHI and EcoRI enzymes. The trasnporters were
187 PCR amplified and digested with BamHI and EcoRI. Both p42K-GPD1p-CYC1t and the
188 transporters were ligated with T4 ligase according to manufacturer's protocol. All plasmid
189 was transformed into *E. coli* DH5α for propagation and maintenance. SR8D8 yeast strain
190 was grown on YPE medium for transformation. SR8D8 transformations were performed
191 using LiAc method according to Gietz *et al.* (Gietz and Schiestl, 2007). Transformants
192 were selected on YPE plate supplemented with 200 µg/ml of geneticin. *At*SWEET1 and
193 *At*SWEET mutants were synthesized as gBlocks and cloned into p42K-GPD1p-CYC1t as
194 described before (Integrated DNA technologies, IA, USA). Variants of LST1_205437
195 mutant were synthesized from Twist Biosciences (Twist Biosciences, CA, USA) and
196 cloned as previously described.
197
198 **2.3 ^{14}C labeled sugar uptake assay**
199 SR8D8 containing the respective plasmid was grown on selective YPE medium to
200 an OD600 of 1-1.5, harvested by centrifugation, and washed twice in ice-cold uptake
201 buffer (100 mM potassium phosphate, pH 6.5). ^{14}C labeled sugar uptake assay was done
202 according to Boles and Oreb (Boles and Oreb, 2018). Radioactivity was analyzed in a
203 Beckman-Coulter LS6500 multi-purpose liquid scintillation counter (Beckman-Coulter,
204 CA, USA).
205 Uptake was measured at sugar concentrations 0.2, 1, 5, 25, and 100 mM for glucose
206 and 1, 5, 25, 66, 100, 200, and 500 mM for xylose. Inhibition of xylose uptake by glucose

was measured at 25, 66, and 100 mM xylose with additional 25 and 100 mM unlabeled glucose. Sugar solutions contained 0.135–0.608 µCi of D-[U-^{14}C]-glucose (290-300 mCi/mmol) or D-[1-^{14}C]-xylose (55 mCi/mmol) (PerkinElmer, MA, USA). Calculation of K_m (Michaelis constant), V_{max} (maximal initial uptake velocity), and K_i (inhibitor constant for competitive inhibition) was done by nonlinear regression analysis and global curve fitting in Prism 7 (GraphPad Software) with values of three independent measurements.

2.4 Transporter identification

Orthologs of known sugar transporters were identified in *R. toruloides* and *L. starkeyi* using BlastP (Altschul et al., 1990). Glucose transporters from *S. cerevisiae* (Hxt7, Hxt2, Hxt1, Hxt3) (Lewis and Bisson, 1991; Ozcan and Johnston, 1999) and xylose transporters from *P. stipitis* (Xut5, Xut2, Rgt2, Xut3) (Jeffries et al., 2007) were used as query sequences for blast search. Search results were filtered by e-value and gene regulation. MEGA X 10.0.1 tool (Kumar et al., 2016) was used to perform ClustalW alignment for the filtered putative sugar transporters and identify conserved structural domains and amino acid residues. The alignment results were edited using the Jalview 2.8 tool (Waterhouse et al., 2009) for enhanced visual presentation.

2.5 Transporter modeling

The homology models of ScGal2, LST_205437, *At*SWEET1 and *At*SWEET7 were constructed using Modeller (Fiser and Sali, 2003). The OF and IF models of Scal2 and LST_205437 were built using the structural template XylE (PDB ID: 4GBZ and 4JA4) (Quistgaard et al., 2013; Sun et al., 2012). The 3D coordinates of XylE structures are

obtained from protein databank. The structural models of OC and OF states of *At*SWEET1 and *At*SWEET7 are obtained using MD predicted structures of OsSWEET2b as template (Selvam et al., 2019). The IF *Os*SWEET2b (Tao et al., 2015) was used to build both *At*SWEET1 and *At*SWEET7 IF models. Molecular docking was performed using Autodock software package (Morris et al., 2009). The PDBQT format files for protein and substrate molecules were obtained using AutoDock Tools. The grid files were generated using Autogrid4 and docking was performed using Autodock4 (Morris et al., 2009). The docking files were visualized using pymol (The PyMOL Molecular Graphics System, Version 1.7, Schrodinger, 2015).

3. Results

3.1 Identification of putative xylose transporters in *Rhodosporidium toruloides* and *Lipomyces starkeyi*

We used knowledge of existing yeast sugar transporters to identify sugar transporters in *R. toruloides* and *L. starkeyi,* which have not been searched for sugar transporters. We found multiple orthologs to HXT transporters from *S. cerevisiae* and XUT transporters from *P. stipitis*. We filtered the transporters with 12 TM domains and conserved sequence motifs (**Fig. 2a**) (Leandro et al., 2009). Recent studies have shown the involvement of the conserved motif G[G/F]XXXG (Young et al., 2014), and Thr213 and Asn370 residues (Farwick et al., 2014) in Hxt7 towards xylose specificity. As such, we used these conserved motifs and residues to refine glucose and xylose specific transporters in *R. toruloides* and *L. starkeyi*. For *L. starkeyi*, LST1_106361 and LST1_205437 were identified as putative glucose transporters and LST1_76 was

identified as a putative xylose transporter. For *R. toruloides*, RTO4_11075 and RTO4_13042 were identified as putative glucose transporters, and RTO4_13731 and RTO4_10452 were identified as putative xylose transporters (**Fig. 2c**). The protein IDs' were picked from respective gene models at JGI mycocosm (Farwick et al., 2014; Young et al., 2014).

3.2 Screening of *Arabidopsis thaliana* SWEET and oleaginous yeast transporters for glucose or xylose transport

It has been well reported that SWEETs transport different sugars, which encouraged us to examine xylose and glucose transport capabilities of 17 *At*SWEET1-17. We used an engineered *S. cerevisiae* strain (SR8D8) capable of xylose fermentation which lacks the Hxt1-7 and Gal2 transporters—rendering it unable to grow on glucose or xylose—for the examination (Kim et al., 2013; Xu, 2015). We measured growth kinetics of SR8D8 transformants expressing the *A. thaliana* SWEETs and putative oleaginous yeast transporters using glucose and xylose as a sole sugar (**Fig. 2b, Fig 2c, and Fig 3**). *Sc*Gal2 expressing SR8D8 was used as a positive control. Most of the SR8D8 transformants expressing *At*SWEETs and putative oleaginous transporter were not able to grow on glucose or xylose. Only *At*SWEET4, *At*SWEET7, and LST1_205437 expressing strains exhibited robust growth on xylose and glucose (**Fig. 3a**).

3.3 *A. thaliana* SWEET and *L. starkeyi* LST1_205437 transporters conferred glucose and xylose cofermentation ability in engineered yeast

To test if the selected transporters can enable consumption of both sugars simultaneously upon introduction to the SR8D8 strain, we performed flask fermentations with a mixture of glucose and xylose and monitored sugar consumption over time. We used the SR8D8 expressing *GAL2* as a baseline control for determining co-consumption phenotypes, because it is known to transport both glucose and xylose in a sequential manner (**Fig. 4a**). In addition, we included *At*SWEET1 as an additional control for *At*SWEETs, because it is most studied SWEET transporter and confers growth of SR8D8 on glucose (**Fig S1a**) (Chen et al., 2010; Cheng et al., 2019a; Eom et al., 2015). Both *At*SWEET4 and *At*SWEET7 showed simultaneous co-utilization of glucose and xylose with different rates within 24 hours. While *At*SWEET1 showed a complete preference for glucose with negligible xylose consumption (**Fig S1a**), *At*SWEET4 showed co-consumption of glucose and xylose with a faster glucose consumption rate than that of xylose (**Fig S1b**). Interestingly, *At*SWEET7 enabled simultaneous co-consumption of glucose and xylose with almost same rates of sugar consumption (**Fig. 4c**). LST1_205437 transporter from *L. starkeyi* showed co-consumption of glucose and xylose (**Fig. 4b**) but glucose consumption was faster than xylose consumption. In further experiments, we chose *At*SWEET1 as a sole glucose transporter, *At*SWEET7 as a glucose and xylose co-transporter, and LST1_205437 as a semi glucose and xylose co-transporter. *At*SWEET7 transports both sugars simultaneously, but suffer from slow transport capacity. While LST1_205437 performs partial co-consumption, it has an efficient transport capacity for both glucose and xylose. The difference could be attributed to the structure and function of the transporters within the isolated organism.

Next, we evaluated fermentation performances of the SR8D8 transformants expressing *At*SWEET1, *At*SWEET7 and LST1_205437 under glucose or xylose conditions (**Fig S2**). As expected, *At*SWEET7 and LST1_205437 transporters enabled glucose and xylose fermentation, depleting all provided sugars. In contrast, *At*SWEET1 enabled robust glucose fermentation but inefficient xylose fermentation with only 5 g/L of xylose consumption within 50 h.

3.4 Kinetic and molecular properties of *A. thaliana* SWEET7 and *L. starkeyi* LST1_205437

To understand kinetic and molecular basis of *At*SWEET7 and LST1_205437 glucose and xylose co-transport phenotypes, we performed radiolabeled sugar transport kinetics experiments, and *in silico* molecular modeling simulations with *Sc*Gal2 and *At*SWEET1 served as representative controls. *Sc*Gal2 was confirmed to be a high affinity glucose transporter (K_M = 1.613 mM, V_{max} = 38.33 nmol/min-mg), with low affinity toward xylose (K_M = 320.5 mM) (**Fig S3c, and Table 1**). Glucose transport kinetics of LST1_205437 was inferior to the *Sc*Gal2 transporter (K_M = 4.975 mM, V_{max} = 46.89 nmol/min-mg), whereas xylose kinetics was superior (K_M = 145.3 mM, V_{max} = 76.8 nmol/min-mg) (**Fig S3e, and Table 1**). These transport kinetic differences were not noticeable during sole sugar fermentation, unlike mixed sugar fermentation (**Fig S2a-2b**).

We then compared transport kinetic properties of *At*SWEET1 and *At*SWEET7. The results showed that *At*SWEET1 transports glucose more efficiently as compared to *At*SWEET7, with very poor xylose transport kinetics (**Fig S3b and S3d**). These kinetics

results of *At*SWEET1 and *At*SWEET7 are consistent with the fermentation results (**Fig S2a-2b**) by the SR8D8 strains expressing *At*SWEET1 and *At*SWEET7.

Individual sugar uptake kinetics results of LST1_205437 supported the partial glucose and xylose co-consumption phenotype. However, the engineered yeast expressing AtSWEET7 showed apparent co-consumption of glucose and xylose, while kinetics results indicated discrepancies in K_M (K_M=75mM for glucose and K_M=308mM) (Table 1). These results prompted us to directly investigate the xylose transport rates by *Sc*Gal2, LST1_205437 and *At*SWEET7 in the presence of glucose. We performed xylose uptake assay with 25 mM or 100 mM glucose, similar conditions that were used in previous study (Farwick et al., 2014). As shown in **Fig. 4d**, xylose transport by *Sc*Gal2 was completely inhibited in the presence of glucose (K_i = 2.3 mM). This kinetic behavior of *Sc*Gal2 is consistent with the mixed sugar fermentation result (**Fig. 4a**). Interestingly, xylose transport by LST1_205437 was less inhibited by glucose than those by *Sc*Gal2 (K_i = 26.7 vs 2.3 mM) (**Fig. 4e**). As a result, the LST1_205437 expressing strain showed a partial co-consumption of glucose and xylose (**Fig. 4b**). Remarkably, *At*SWEET7 showed no inhibition of xylose transport by glucose (**Fig. 4f, Table 1**) (**Fig. 4c**). Next, we performed a mixed sugar fermentation experiment under industrially-relevant sugar concentrations of 7 % glucose and 4 % xylose to validate co-fermentation of AtSWEET7 and LST1_205437. As expected the *Sc*Gal2 expressing strain exhibited a sequential utilization of glucose and xylose (Fig. 5a). The sugar utilization profile of the LST1_20437 expressing strain was consistent with the kinetics data, showing partial xylose and glucose co-consumption (Fig. 5b). The AtSWEET7 expressing strain showed co-consumption of glucose and xylose even at higher glucose concentrations, further

supporting that AtSWEET7 is indeed glucose and xylose co-transporter which is insensitive to glucose inhibition even under high glucose concentrations (Fig. 5c).

To probe critical amino-acid residues responsible for the observed phenotypes—severe and partial glucose inhibition on xylose—of *Sc*Gal2 and LST1_205437, we performed *in-silico* docking studies to predict the preferred binding sites of glucose and xylose in *Sc*Gal2 and LST1_205437. We constructed the homology models of outward-facing (OF) and inward facing (IF) states of *Sc*Gal2 and LST1_205437 using the closest homologous structure, XylE (Quistgaard et al., 2013; Sun et al., 2012) and docked glucose and xylose into the primary binding site (see Methods for details) (**Fig. 6 and Fig S4-5**). Glucose and xylose exhibited conserved binding mode in *Sc*Gal2 and LST1_205437 in OF states and our docked pose shows close match with previous studies based on XylE (Sun et al., 2012) (**Fig. 6a-6d**). The non-conserved residue Tyr446 in *Sc*Gal2 is involved in hydrogen bond interaction with both substrates while the equivalent residue Phe433 in LST1_205437 does not form any polar interaction. The presence of additional hydroxylmethyl moiety in glucose forms favorable contact with Thr219 (ScGal2)/Thr209 (LST1_205437) and stabilizes glucose in the binding site. However, striking differences were observed in the binding mode of substrate molecules in the IF state (**Fig. 6e-6h**). The structural transition to IF state exposes Asn346 (*Sc*Gal2) to the binding site and plays crucial role in substrate translocation. Both glucose and xylose were involved in hydrogen bond interaction with Tyr446 and Asn346 in *Sc*Gal2. In contrast, the equivalent residues Phe433 and Ala335 in LST1_205437 cannot form hydrogen bond interaction with glucose and xylose. Furthermore, dynamics involving both N- and C-terminal domains in LST1_205437 leads to co-transport of both glucose and

xylose. In contrast xylose fails to form favorable contact with N-domain residues in ScGal2 which may be required for efficient transport. To validate the docking results, we constructed the SR8D8 expressing LST1_205437 with Ala335Asn mutation (LST1_205437_A335N) and examined the profile of glucose and xylose utilization. As expected, the Ala335Asn mutation of LST1_205437 increased glucose uptake and decreased the xylose uptake as compared to the wild type (**Fig S6**).

In contrast to *Sc*Gal2 and LST1_205437 with 12 TM domains, *At*SWEET7 with 7 TM domains showed no inhibition of xylose transport in the presence of either 25 mM or 100 mM glucose (**Fig. 4f and Table 1**). This unique kinetic properties of *At*SWEET7 are consistent with the fermentation result (**Fig. 4c and Fig 5c**). Both *At*SWEET1 and *At*SWEET7 are structurally related to each other, but when expressed in SR8D8 they showed different mixed-sugar fermentation phenotypes (**Fig S7**). The *At*SWEET1 expressing strain consumed glucose rapidly but did not utilize xylose (**Fig S1a**). The *At*SWEET7 expressing strain consumed glucose and xylose simultaneously (**Fig. 4c**). In a previous study, we characterized the complete glucose transport cycle in *Os*SWEET2b using molecular dynamics (MD) simulations (Selvam et al., 2019). Using the MD predicted structures of the occluded (OC) and OF states as structural templates, we constructed the homology models of intermediate conformations of *At*SWEET1 and *At*SWEET7 (**Fig S8**) (Selvam et al., 2019). The IF models were built using an *Os*SWEET2b crystal structure (Tao et al., 2015). The substrate molecules were docked in three different states and bound poses were predicted to be similar in both *At*SWEET1 and *At*SWEET7 (**Fig. 7 and Fig S9**). However, the major differences between *At*SWEET1 and *At*SWEET7 were observed in the non-conserved residues that stabilize the glucose and xylose in the

binding site. The docking results reveals that substrate molecules are sandwiched between Trp59 and Trp183 in *At*SWEET7 while the equivalent residues in *At*SWEET1 are Ser54 and Trp176 cannot form a strong stacking interaction with substrates (**Fig. 7**). Molecular simulations have also shown that the presence of two bulky aromatic residues in the binding site of bacterial SemiSWEET with one THB decreases the substrate dynamics and thereby increases the energetic barrier for substrate transport (28). Similarly, the non-conserved residues Asn145 (Ser138) and Asn179 (Cys172) in *At*SWEET7 have an extended amide group that forms favorable contact with both substrates in all three major conformational states (**Fig. 7**) whereas the counterpart residues Ser138 and Cys172 in *At*SWEET1 cannot form favorable interactions in all the conformational states. To validate our findings, we mutated Trp59Ser in *At*SWEET7 and observed decreased xylose transport without affecting the glucose uptake (**Fig S10d**). We also identified secondary hydrophobic gating residues in our previous study and mutating of one of the hydrophobic residues beneath these gating residues Phe168Ala in *At*SWEET1 improves the glucose transport and allows the co-transport of xylose (**Fig S9, and S10c**).

3.5 Alteration of Asn365 amino acid residue in *L. starkeyi* LST1_205437 changes sugar preference

Asn370/376 residues in *S. cerevisiae* hexose transporters Gal2 and Hxt7 play a critical role in glucose and xylose co-transport (Farwick et al., 2014). Replacing the Asn370/376 residue in Gal2 and Hxt7 with either hydrophobic or hydrophilic amino acids led to alleviation of glucose inhibition on xylose transport (Farwick et al., 2014). Interestingly, LST1_205437 transporter retains Asn365 (equivalent to Asn370 in Gal2)

411 residue and show partial inhibition of xylose uptake by glucose (**Fig. 4b and 4e**). We
412 sought to test if alteration of Asn365 residue in LST1_205437 to phenylalanine, serine or
413 valine would further alleviate glucose inhibition on xylose transport, allowing complete co-
414 fermentation of glucose and xylose. We found that Asn365Phe, Asn365Ser, and
415 Asn365Val mutations in LST1_205437 resulted in similar phenotypic changes as it was
416 reported by Farwick e*t al*. Particularly, Asn365Phe mutation abolished glucose transport
417 while retaining xylose, Asn365Ser and Asn365Val showed co-fermentation phenotypes
418 (**Fig. 8b-8d**). Our computational investigation also showed that Asn365 mutation to
419 phenylalanine sterically hinders the binding mode of the glucose molecule and hence
420 results in loss of transport function (**Fig. 7e**). Altogether Asn365 residue mutation
421 functions not only in *S. cerevisiae* transporters but also in *L. starkeyi* LST1_205437,
422 supporting the universal importance of Asn370/376 residue in closely related yeast
423 hexose transporters.
424
425 **4. Discussion**
426 The wealth of sequencing information and recently discovered SWEET family sugar
427 transporters are still unexplored by bioprospecting for tackling glucose and xylose co-
428 transport problem. In this study, we undertook a bioprospecting approach to identify
429 glucose and xylose co-transporting transporters from unexplored oleaginous yeasts and
430 plant (**Fig. 1**). We identified 8 putative xylose transporters in *R. toruloides* and *L. starkeyi*
431 (**Fig. 2c**). However, experimental validation of the putative transporters using a xylose-
432 fermenting *S. cerevisiae* lacking major hexose transporters (SR8D8) showed that only *L.*
433 *starkeyi* LST1_205437 can enable robust growth on either glucose or xylose (**Fig. 3a**).

Interestingly, LST1_205437 retained conserved Thr213 and Asn370 residues, and demonstrated a partial cofermentation of glucose and xylose (**Fig. 4b**). Furthermore, the glucose inhibition kinetics by LST_205437 showed less glucose inhibition on xylose transport whereas *Sc*Gal2 exhibited severe glucose inhibition on xylose transport even under a low glucose concentration (25mM) (**Fig. 4d, and 4e**). This observation provides evidence that other than Thr213 and Asn370 residues might be involved in the partial cofermentation phenotype. *In silico* analysis reveals that the non-conserved residues Tyr446/Phe433 and Asn346/Ala335 might play crucial role in substrate binding and transport in *Sc*Gal2 and LST1_205437 (**Fig. 6**). The increase in polarity restricts the binding of xylose only to C-terminus in *Sc*Gal2; however, dynamics involving both C and N domains is essential for efficient transport of both glucose and xylose in LST1_205437. The fermentation experiments also support our prediction and mutation of Ala335Asn decreases the xylose uptake in LST1_205437.

Most studies related to xylose transporters focused on MFS (**M**ajor **F**acilitator **S**uperfamily) type transporters with 12 TM domains, and other families of sugar transporters have been overlooked. Here, we expanded bioprospecting approach toward SWEET family transporters. *A. thaliana* has 17 SWEET transporters that can transport either monosaccharides or disaccharides across a membrane via concentration gradients (**Fig. 2b**) (Chen et al., 2015). According to Han *et. al. A. thaliana* SWEETs can be divided into two distinct groups based on conserved residues dictating sugar preference to monosaccharide or disaccharide. However, the authors discovered that this division could not reflect sugar specificity for all *At*SWEETs. In particular, Han *et al.* showed that *At*SWEET13 have both glucose and sucrose transport activities (Han et al., 2017).

Therefore, in this study, we screened all 17 *At*SWEETs to identify xylose and glucose transporter. Interestingly, 17 *At*SWEETs share sequence similarity and yet showed very different sugar uptake phenotypes on glucose or xylose. We confirmed *At*SWEET1 to be a glucose transporter with almost no xylose transport capacity, whereas *At*SWEET4 and *At*SWEET7 showed both glucose and xylose transport capacities (**Fig S1 and Fig. 4c**). Moreover, among screened transporters, *At*SWEET7 exhibited complete co-fermentation phenotype. The kinetic analysis of *At*SWEET7 revealed no glucose inhibition of xylose transport, though the glucose and xylose transport kinetic properties were poorer than *Sc*Gal2 and LST_205437 (**Fig. 4f and Fig S3**). Moreover, AtSWEET7 exhibited complete co-fermentation of glucose and xylose even at high residual glucose concentrations, suggesting the transporter is completely insensitive to glucose inhibition (**Fig. 5c**). Recently, Podolsky *et al.,* demonstrated utility of fungal SWEET transporters to tackle glucose and xylose cotransport problem. The authors demonstrated that the wild-type NcSWEET1 and the best performing chimera derived from it allowed co-transport of glucose and xylose. However, in their experimental setup *S. cerevisiae* expressing wild type and the chimera transporter co-consumed only 20 g/L of sugars within 120 hours (Podolsky et al., 2021). Similar results were achieved in engineered Asn366Thr Hxt11 transporter, which belongs to MFS family, engineering of native glucose and xylose co-transporter with more simpler molecular structure than MFS might be advantageous for transporter engineering (Shin et al., 2015).

More recently, we investigated the glucose transport cycle in *Os*SWEET2b and Bacterial SemiSWEET with 3 TMs and reported that substrate transport mechanism varies between closely related families of transporters (Selvam et al., 2019). We

480 constructed the homology models of *At*SWEET1 and *At*SWEET7 intermediate states and
481 docked the substrate in the binding site (**Fig. 7 and Fig S9**). The results revealed that the
482 substrate molecules were sandwiched between Trp59 and Trp183 in *At*SWEET7, thereby
483 enables the structural transition to other states for efficient transport. The lack of one of
484 the aromatic counterpart may lead to the increase in conformation degrees of rotational
485 freedom that could possibly affects the substrate stability in the binding site and the
486 transport (Cheng et al., 2019a). As expected, the mutation of Trp59 decreased the xylose
487 transport in *At*SWEET7 (**Fig S10d**). In a previous study, we identified a hydrophobic gate
488 at the center of transporter and opening of these gates drives the conformational
489 transition of IF state (Selvam et al., 2019). In *At*SWEET1, Phe169 is located just beneath
490 the hydrophobic gates and the mutation of this residue to alanine increases the glucose
491 uptake and shows partial cotransport of xylose (**Fig S10c**). Although SWEETs transport
492 both glucose and xylose via the same translocation pore, the free energy barriers and the
493 critical residues that facilitate the transport along the pore cavity could be different.
494 Extensive long timescale simulations are required to characterize the mechanistic
495 difference between glucose and xylose transport that provides more insights into atomic-
496 level details of the transport mechanism.
497
498 **5. Conclusion**
499 In summary, this work demonstrates how bioprospecting can identify unique
500 transporters for industrial applications. Availability of vast amounts of sequencing
501 information, allowed us to identify and characterize yeast transporter LST_205437 that
502 has partial glucose and xylose co-consumption capacity. We found that LST_205437 has

non conserved amino acid residue responsible for the phenotype. We characterized newly discovered SWEET transporters, which are structurally different from its yeast counterparts. Using *in silico* modeling, we were able to identify key amino acid residues responsible for glucose and xylose co-transport. The discovered data could be further used for rational transporter engineering of *At*SWEETs and yeast transporters to improve xylose and glucose transport characteristics. Altogether, information gathered in this study will increase the understanding of yeast hexose transporters and SWEET transporters, providing valuable information for industrial biotechnology and fundamental biology.

6. Data Availability Statement

Data available on request from the authors.

7. Author contributions

N.K., L.C., D.S., C.R., and Y.J. conceived and designed the study. N.K., S.J, and J.L., performed experiments. A.D. performed bioinformatics analysis. B.S. performed *in silico* studies and docking analysis. N.K., and Y.J. analyzed and interpreted the data and wrote the manuscript in discussion with all authors.

8. Acknowledgements

This material is based on the work supported by the US Department of Energy, Office of Science, Office of Biological and Environmental Research under Award Number(s) DE-SC0018420. We thank Blue Waters Supercomputing Facility funded by National Science

Foundation (OCI-0725070 and ACI-1238993) and the state of Illinois for the computer time. D.S acknowledges New Innovator Award from the Foundation for Food and Agricultural Research (FFAR) and NSF Early CAREER Award, NSF MCB 18-45606 for the research support.

9. Competing interests

The Authors declare that there is no conflict of interest

10. References

Adrio, J.L., (2017) Oleaginous yeasts: Promising platforms for the production of oleochemicals and biofuels. Biotechnol Bioeng 114, 1915-1920.

Altschul, S.F., Gish, W., Miller, W., Myers, E.W., Lipman, D.J., (1990) Basic local alignment search tool. J Mol Biol 215, 403-410.

Boles, E., Oreb, M., (2018) A Growth-Based Screening System for Hexose Transporters in Yeast. Methods Mol Biol 1713, 123-135.

Brat, D., Boles, E., Wiedemann, B., (2009) Functional expression of a bacterial xylose isomerase in Saccharomyces cerevisiae. Appl Environ Microbiol 75, 2304-2311.

Carroll, A., Somerville, C., (2009) Cellulosic biofuels. Annu Rev Plant Biol 60, 165-182.

Chen, L.Q., Cheung, L.S., Feng, L., Tanner, W., Frommer, W.B., (2015) Transport of sugars. Annu Rev Biochem 84, 865-894.

Chen, L.Q., Hou, B.H., Lalonde, S., Takanaga, H., Hartung, M.L., Qu, X.Q., Guo, W.J., Kim, J.G., Underwood, W., Chaudhuri, B., Chermak, D., Antony, G., White, F.F., Somerville, S.C., Mudgett, M.B., Frommer, W.B., (2010) Sugar transporters for intercellular exchange and nutrition of pathogens. Nature 468, 527-532.

Cheng, K.J., Selvam, B., Chen, L.Q., Shukla, D., (2019a) Distinct Substrate Transport Mechanism Identified in Homologous Sugar Transporters. J Phys Chem B 123, 8411-8418.

Cheng, M.H., Dien, B.S., Lee, D.K., Singh, V., (2019b) Sugar production from bioenergy sorghum by using pilot scale continuous hydrothermal pretreatment combined with disk refining. Bioresour Technol 289, 121663.

Coradetti, S.T., Pinel, D., Geiselman, G.M., Ito, M., Mondo, S.J., Reilly, M.C., Cheng, Y.F., Bauer, S., Grigoriev, I.V., Gladden, J.M., Simmons, B.A., Brem, R.B., Arkin, A.P., Skerker, J.M., (2018) Functional genomics of lipid metabolism in the oleaginous yeast Rhodosporidium toruloides. Elife 7.

Eom, J.S., Chen, L.Q., Sosso, D., Julius, B.T., Lin, I.W., Qu, X.Q., Braun, D.M., Frommer, W.B., (2015) SWEETs, transporters for intracellular and intercellular sugar translocation. Curr Opin Plant Biol 25, 53-62.

Farwick, A., Bruder, S., Schadeweg, V., Oreb, M., Boles, E., (2014) Engineering of yeast hexose transporters to transport D-xylose without inhibition by D-glucose. Proc Natl Acad Sci U S A 111, 5159-5164.

564 Fiser, A., Sali, A., (2003) Modeller: generation and refinement of homology-based protein structure
565 models. Methods Enzymol 374, 461-491.
566 Gardonyi, M., Jeppsson, M., Liden, G., Gorwa-Grauslund, M.F., Hahn-Hagerdal, B., (2003) Control of
567 xylose consumption by xylose transport in recombinant Saccharomyces cerevisiae. Biotechnol Bioeng
568 82, 818-824.
569 Gietz, R.D., Schiestl, R.H., (2007) High-efficiency yeast transformation using the LiAc/SS carrier DNA/PEG
570 method. Nat Protoc 2, 31-34.
571 Ha, S.J., Galazka, J.M., Kim, S.R., Choi, J.H., Yang, X., Seo, J.H., Glass, N.L., Cate, J.H., Jin, Y.S., (2011)
572 Engineered Saccharomyces cerevisiae capable of simultaneous cellobiose and xylose fermentation. Proc
573 Natl Acad Sci U S A 108, 504-509.
574 Hamacher, T., Becker, J., Gardonyi, M., Hahn-Hagerdal, B., Boles, E., (2002) Characterization of the
575 xylose-transporting properties of yeast hexose transporters and their influence on xylose utilization.
576 Microbiology 148, 2783-2788.
577 Han, L., Zhu, Y., Liu, M., Zhou, Y., Lu, G., Lan, L., Wang, X., Zhao, Y., Zhang, X.C., (2017) Molecular
578 mechanism of substrate recognition and transport by the AtSWEET13 sugar transporter. Proc Natl Acad
579 Sci U S A 114, 10089-10094.
580 Jeena, G.S., Kumar, S., Shukla, R.K., (2019) Structure, evolution and diverse physiological roles of SWEET
581 sugar transporters in plants. Plant Mol Biol 100, 351-365.
582 Jeffries, T.W., Grigoriev, I.V., Grimwood, J., Laplaza, J.M., Aerts, A., Salamov, A., Schmutz, J., Lindquist, E.,
583 Dehal, P., Shapiro, H., Jin, Y.S., Passoth, V., Richardson, P.M., (2007) Genome sequence of the
584 lignocellulose-bioconverting and xylose-fermenting yeast Pichia stipitis. Nat Biotechnol 25, 319-326.
585 Jeffries, T.W., Jin, Y.S., (2004) Metabolic engineering for improved fermentation of pentoses by yeasts.
586 Appl Microbiol Biotechnol 63, 495-509.
587 Jin, Y.S., Ni, H., Laplaza, J.M., Jeffries, T.W., (2003) Optimal growth and ethanol production from xylose
588 by recombinant Saccharomyces cerevisiae require moderate D-xylulokinase activity. Appl Environ
589 Microbiol 69, 495-503.
590 Kim, S.R., Ha, S.J., Wei, N., Oh, E.J., Jin, Y.S., (2012) Simultaneous co-fermentation of mixed sugars: a
591 promising strategy for producing cellulosic ethanol. Trends Biotechnol 30, 274-282.
592 Kim, S.R., Skerker, J.M., Kang, W., Lesmana, A., Wei, N., Arkin, A.P., Jin, Y.S., (2013) Rational and
593 evolutionary engineering approaches uncover a small set of genetic changes efficient for rapid xylose
594 fermentation in Saccharomyces cerevisiae. PLoS One 8, e57048.
595 Kotter, P., Amore, R., Hollenberg, C.P., Ciriacy, M., (1990) Isolation and characterization of the Pichia
596 stipitis xylitol dehydrogenase gene, XYL2, and construction of a xylose-utilizing Saccharomyces cerevisiae
597 transformant. Curr Genet 18, 493-500.
598 Kumar, S., Stecher, G., Tamura, K., (2016) MEGA7: Molecular Evolutionary Genetics Analysis Version 7.0
599 for Bigger Datasets. Mol Biol Evol 33, 1870-1874.
600 Kuyper, M., Harhangi, H.R., Stave, A.K., Winkler, A.A., Jetten, M.S., de Laat, W.T., den Ridder, J.J., Op den
601 Camp, H.J., van Dijken, J.P., Pronk, J.T., (2003) High-level functional expression of a fungal xylose
602 isomerase: the key to efficient ethanolic fermentation of xylose by Saccharomyces cerevisiae? FEMS
603 Yeast Res 4, 69-78.
604 Kwak, S., Jin, Y.S., (2017) Production of fuels and chemicals from xylose by engineered Saccharomyces
605 cerevisiae: a review and perspective. Microb Cell Fact 16, 82.
606 Leandro, M.J., Fonseca, C., Goncalves, P., (2009) Hexose and pentose transport in ascomycetous yeasts:
607 an overview. FEMS Yeast Res 9, 511-525.
608 Lewis, D.A., Bisson, L.F., (1991) The HXT1 gene product of Saccharomyces cerevisiae is a new member of
609 the family of hexose transporters. Mol Cell Biol 11, 3804-3813.
610 Li, H., Schmitz, O., Alper, H.S., (2016) Enabling glucose/xylose co-transport in yeast through the directed
611 evolution of a sugar transporter. Appl Microbiol Biotechnol 100, 10215-10223.

612 Morris, G.M., Huey, R., Lindstrom, W., Sanner, M.F., Belew, R.K., Goodsell, D.S., Olson, A.J., (2009)
613 AutoDock4 and AutoDockTools4: Automated docking with selective receptor flexibility. J Comput Chem
614 30, 2785-2791.
615 Ozcan, S., Johnston, M., (1999) Function and regulation of yeast hexose transporters. Microbiol Mol Biol
616 Rev 63, 554-569.
617 Parachin, N.S., Bergdahl, B., van Niel, E.W., Gorwa-Grauslund, M.F., (2011) Kinetic modelling reveals
618 current limitations in the production of ethanol from xylose by recombinant Saccharomyces cerevisiae.
619 Metab Eng 13, 508-517.
620 Podolsky, I.A., Seppala, S., Xu, H., Jin, Y.S., O'Malley, M.A., (2021) A SWEET surprise: Anaerobic fungal
621 sugar transporters and chimeras enhance sugar uptake in yeast. Metab Eng.
622 Quistgaard, E.M., Low, C., Moberg, P., Tresaugues, L., Nordlund, P., (2013) Structural basis for substrate
623 transport in the GLUT-homology family of monosaccharide transporters. Nat Struct Mol Biol 20, 766-
624 768.
625 Reider Apel, A., Ouellet, M., Szmidt-Middleton, H., Keasling, J.D., Mukhopadhyay, A., (2016) Evolved
626 hexose transporter enhances xylose uptake and glucose/xylose co-utilization in Saccharomyces
627 cerevisiae. Sci Rep 6, 19512.
628 Riley, R., Haridas, S., Wolfe, K.H., Lopes, M.R., Hittinger, C.T., Goker, M., Salamov, A.A., Wisecaver, J.H.,
629 Long, T.M., Calvey, C.H., Aerts, A.L., Barry, K.W., Choi, C., Clum, A., Coughlan, A.Y., Deshpande, S.,
630 Douglass, A.P., Hanson, S.J., Klenk, H.P., LaButti, K.M., Lapidus, A., Lindquist, E.A., Lipzen, A.M., Meier-
631 Kolthoff, J.P., Ohm, R.A., Otillar, R.P., Pangilinan, J.L., Peng, Y., Rokas, A., Rosa, C.A., Scheuner, C., Sibirny,
632 A.A., Slot, J.C., Stielow, J.B., Sun, H., Kurtzman, C.P., Blackwell, M., Grigoriev, I.V., Jeffries, T.W., (2016)
633 Comparative genomics of biotechnologically important yeasts. Proc Natl Acad Sci U S A 113, 9882-9887.
634 Sedlak, M., Ho, N.W., (2004) Characterization of the effectiveness of hexose transporters for
635 transporting xylose during glucose and xylose co-fermentation by a recombinant Saccharomyces yeast.
636 Yeast 21, 671-684.
637 Selvam, B., Yu, Y.C., Chen, L.Q., Shukla, D., (2019) Molecular Basis of the Glucose Transport Mechanism
638 in Plants. ACS Cent Sci 5, 1085-1096.
639 Shin, H.Y., Nijland, J.G., de Waal, P.P., de Jong, R.M., Klaassen, P., Driessen, A.J., (2015) An engineered
640 cryptic Hxt11 sugar transporter facilitates glucose-xylose co-consumption in Saccharomyces cerevisiae.
641 Biotechnol Biofuels 8, 176.
642 Shirkavand, E., Baroutian, S., Gapes, D.J., Young, B.R., (2016) Combination of fungal and physicochemical
643 processes for lignocellulosic biomass pretreatment – A review. Renewable and Sustainable Energy
644 Reviews 54, 217-234.
645 Subtil, T., Boles, E., (2012) Competition between pentoses and glucose during uptake and catabolism in
646 recombinant Saccharomyces cerevisiae. Biotechnol Biofuels 5, 14.
647 Sun, L., Zeng, X., Yan, C., Sun, X., Gong, X., Rao, Y., Yan, N., (2012) Crystal structure of a bacterial
648 homologue of glucose transporters GLUT1-4. Nature 490, 361-366.
649 Tao, Y., Cheung, L.S., Li, S., Eom, J.S., Chen, L.Q., Xu, Y., Perry, K., Frommer, W.B., Feng, L., (2015)
650 Structure of a eukaryotic SWEET transporter in a homotrimeric complex. Nature 527, 259-263.
651 Waterhouse, A.M., Procter, J.B., Martin, D.M., Clamp, M., Barton, G.J., (2009) Jalview Version 2--a
652 multiple sequence alignment editor and analysis workbench. Bioinformatics 25, 1189-1191.
653 Xu, H., (2015) Engineering Saccharomyces cerevisiae for cellulosic ethanol production. Food Science &
654 Human Nutrition. University of Illinois at Urbana-Champaign.
655 Xuan, Y.H., Hu, Y.B., Chen, L.Q., Sosso, D., Ducat, D.C., Hou, B.H., Frommer, W.B., (2013) Functional role
656 of oligomerization for bacterial and plant SWEET sugar transporter family. Proc Natl Acad Sci U S A 110,
657 E3685-3694.
658 Young, E., Poucher, A., Comer, A., Bailey, A., Alper, H., (2011) Functional survey for heterologous sugar
659 transport proteins, using Saccharomyces cerevisiae as a host. Appl Environ Microbiol 77, 3311-3319.

660 Young, E.M., Tong, A., Bui, H., Spofford, C., Alper, H.S., (2014) Rewiring yeast sugar transporter
661 preference through modifying a conserved protein motif. Proc Natl Acad Sci U S A 111, 131-136.
662 Zhang, S., Skerker, J.M., Rutter, C.D., Maurer, M.J., Arkin, A.P., Rao, C.V., (2016) Engineering
663 Rhodosporidium toruloides for increased lipid production. Biotechnol Bioeng 113, 1056-1066.
664 Zhou, H., Cheng, J.S., Wang, B.L., Fink, G.R., Stephanopoulos, G., (2012) Xylose isomerase overexpression
665 along with engineering of the pentose phosphate pathway and evolutionary engineering enable rapid
666 xylose utilization and ethanol production by Saccharomyces cerevisiae. Metab Eng 14, 611-622.

667

Figures and Table legends

Fig. 1: Bioprospecting strategy implemented in this study. This figure depicts the main steps applied to identify novel xylose and glucose co-transporting transporters. **a** Identification transporters from emerging oleaginous yeasts *Lipomyces starkeyi* and *Rhodosporidium toruloides.* **b** Characterization of SWEET transporters from *Arabidopsis thaliana.* **c** Schematic fermentation profile of a sugar mixture containing glucose and xylose by the engineered *S. cerevisiae*. Glucose presence inhibits xylose transport leading to sequential sugar utilization. Application of the discovered transporters relief glucose inhibition of xylose transport, leading to glucose and xylose co-consumption.

Fig. 2: Bioinformatics analysis for transporter identification. a Most monosaccharide transporters in yeasts have 12 TM domains (represented in blue). The conserved motifs identified in yeasts transporters are marked in orange (I-V). Motif X (marked in green) has recently been identified as a key motif involved in xylose specificity. **b** A phylogenetic tree of the 17 *A. thaliana* SWEET transporters clusters the monosaccharide and disaccharide transporters independently. **c** Multiple sequence alignment of putative transporters: Thr213 and Ans370 are conserved in reported glucose transporters in yeasts.

Fig. 3: *L. starkeyi*, *R. toruloides* and *A. thaliana* SWEET transporter screening for growth on glucose or xylose. **a** Growth characteristics of the SR8D8 strain expressing transporters were summarized using a plot with. X axis represents the cell densities on glucose and Y axis represents the cell densities on xylose. Cell densities of the

transporter-expressing strains at 40 hrs were presented. **b** Growth curves of the four strains with an overexpression cassette of *GAL2*, *At*SWEET4, *At*SWEET7, or a control plasmids (SRD8) on xylose and glucose. The dots and line lines are means from duplicated cultures.

Fig. 4: Glucose and xylose mixed sugar fermentation profile and inhibitory effect of glucose on xylose transport. 20 g/L of glucose and xylose mixed sugar fermentation by SR8D8 expressing *Sc*Gal2 (sequential fermentation) (**a**), LST1_205437 (partial cofermentation) (**b**), *At*SWEET7 (true co-fermentation) (**c**). Symbols: glucose (square), xylose (triangle up), DCW (circle). Inhibitory effect of 0 mM, 25 mM and 100 mM glucose on xylose transport in SR8D8 expressing *Sc*Gal2 (**d**), LST1_205437 (**e**) and *At*SWEET7 (**f**). Global curve fitting for Michaelis–Menten kinetics with competitive inhibition was applied to data of three independent measurements at each concentration.

Fig. 5: Glucose and xylose mixed sugar fermentation profile using industrially relevant sugar concentrations. 70 g/L of glucose and 40g/L xylose mixed sugar fermentation by SR8D8 expressing *Sc*Gal2 (**a**), LST1_205437 (**b**), *At*SWEET7 (**c**). Symbols: glucose (square), xylose (triangle up), DCW (circle). The values are the means of two independent experiments, and the error bars indicate the standard errors

Fig. 6: Predicted binding orientation of glucose and xylose in *Sc*Gal2 and LST1_205437. The dock poses of glucose and xylose in OF conformations for

LST1_205437 (**a, c**) and *Sc*Gal2 (**b, d**), respectively. The dock poses of glucose and xylose in IF conformations for LST1_205437 (**e, g**) and *Sc*Gal2 (**f, h**), respectively.

Fig. 7: Dockposes of glucose and xylose in *At*SWEET1 and *At*SWEET7. The predicted binding mode of glucose and xylose in *At*SWEET1 and *At*SWEET7 in OF (**a** and **d**), OC (**b** and **e**) and IF (**c** and **f**) conformations.

Fig. 8: Glucose and xylose mixed sugar fermentation profile of SR8D8 expressing LST1_205437 Asn365 mutant variants and glucose dockpose of LST1_205437 Asn365Phe. LST1_205437 Asn365Phe mutant, LST1_205437 Asn365Ser and LST1_205437 Asn365Val. 20 g/L of glucose and xylose mixed sugar fermentation in YP medium of LST1_205437 wild type (**a**), LST1_205437 Asn365Phe (**b**), LST1_205437 Asn365Ser (**c**) and LST1_205437 Asn365Val (**d**). Mutation of Asn365 to phenylalanine in LST1_205437 (**e**). Asn365 form crucial contact with glucose molecule in stabilize the IF state. The mutation to phenylalanine results in steric clash with substrate and affects the conformational transition to intermediate states and transport. Symbols: glucose (square), xylose (triangle up), DCW (circle). The values are the means of two independent experiments, and the error bars indicate the standard errors

Table 1 Kinetic properties of *Sc*Gal2, *At*SWEET7 and LST1_205437

Figures

Fig. 1

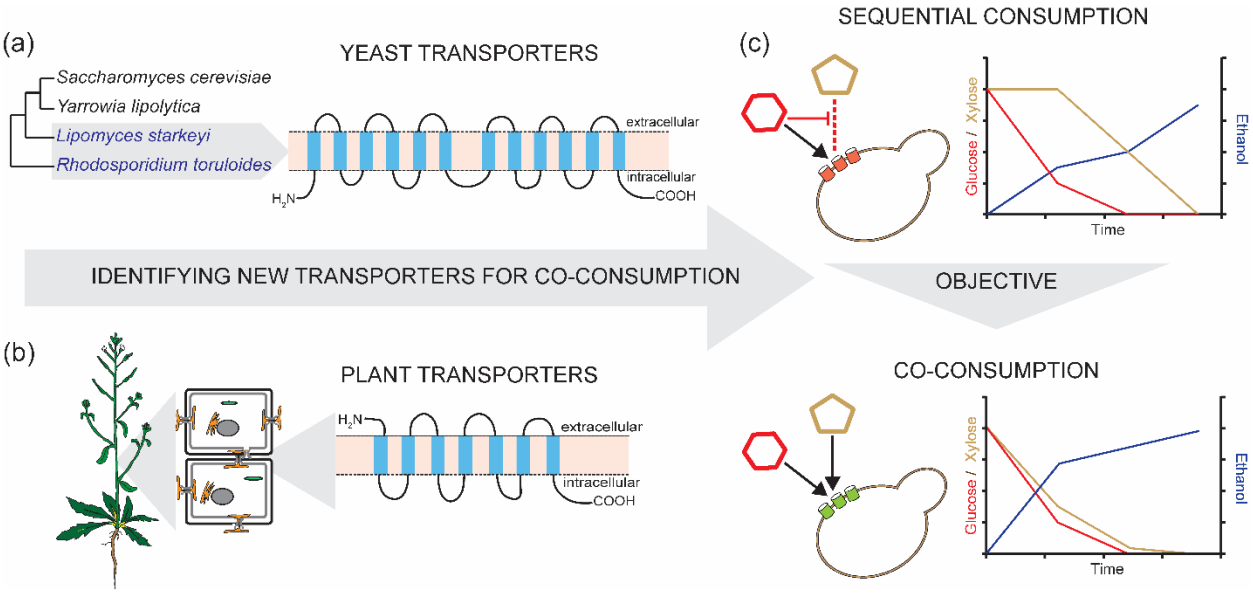

Fig. 1: Bioprospecting strategy implemented in this study. This figure depicts the main steps applied to identify novel xylose and glucose co-transporting transporters. **a** Identification transporters from emerging oleaginous yeasts *Lipomyces starkeyi* and *Rhodosporidium toruloides.* **b** Characterization of SWEET transporters from *Arabidopsis thaliana.* **c** Schematic fermentation profile of a sugar mixture containing glucose and xylose by the engineered *S. cerevisiae*. Glucose presence inhibits xylose transport leading to sequential sugar utilization. Application of the discovered transporters relief glucose inhibition of xylose transport, leading to glucose and xylose co-consumption.

Fig. 2

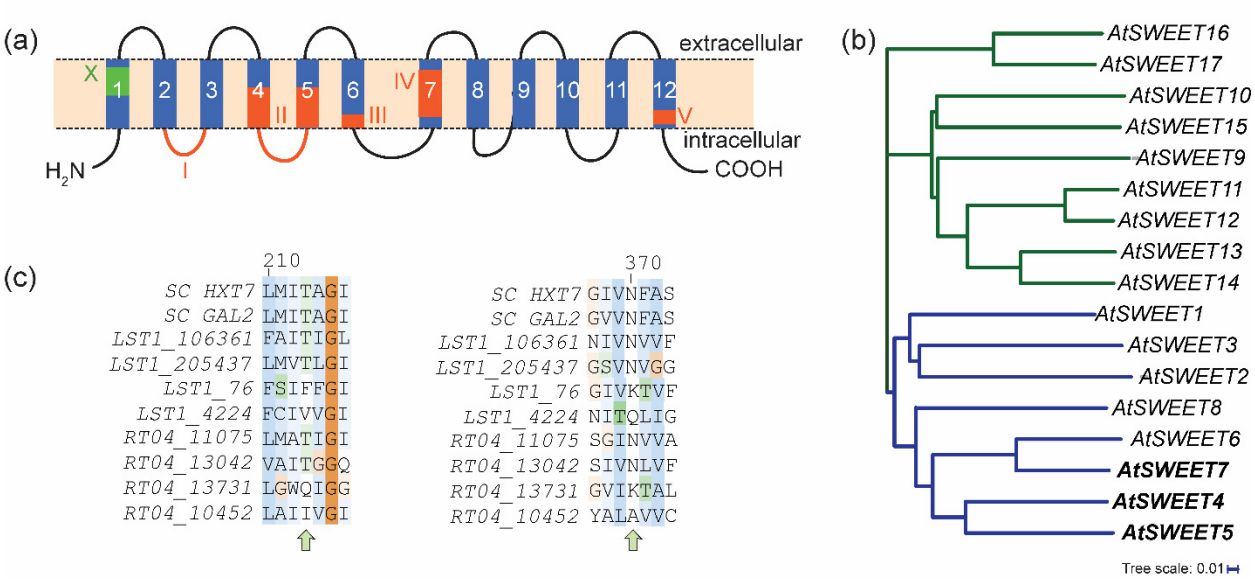

Fig. 2: Bioinformatics analysis for transporter identification. a Most monosaccharide transporters in yeasts have 12 TM domains (represented in blue). The conserved motifs identified in yeasts transporters are marked in orange (I-V). Motif X (marked in green) has recently been identified as a key motif involved in xylose specificity. **b** A phylogenetic tree of the 17 *A. thaliana* SWEET transporters clusters the monosaccharide and disaccharide transporters independently. **c** Multiple sequence alignment of putative transporters: Thr213 and Ans370 are conserved in reported glucose transporters in yeasts.

765 **Fig. 3**

766

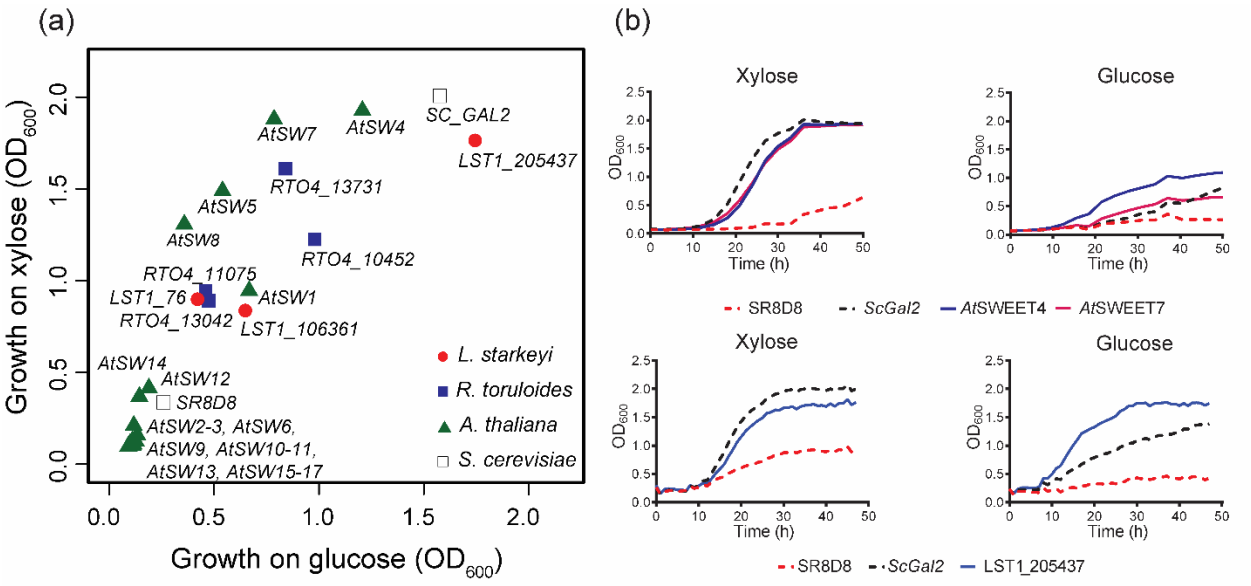

767

768

769 **Fig. 3: *L. starkeyi*, *R. toruloides* and *A. thaliana* SWEET transporter screening for**
770 **growth on glucose or xylose**. **a** Growth characteristics of the SR8D8 strain expressing
771 transporters were summarized using a plot with. X axis represents the cell densities on
772 glucose and Y axis represents the cell densities on xylose. Cell densities of the
773 transporter-expressing strains at 40 hrs were presented. **b** Growth curves of the four
774 strains with an overexpression cassette of *GAL2*, *At*SWEET4, *At*SWEET7, or a control
775 plasmids (SRD8) on xylose and glucose. The dots and line lines are means from
776 duplicated cultures.

777

778

779 **Fig. 4**

780

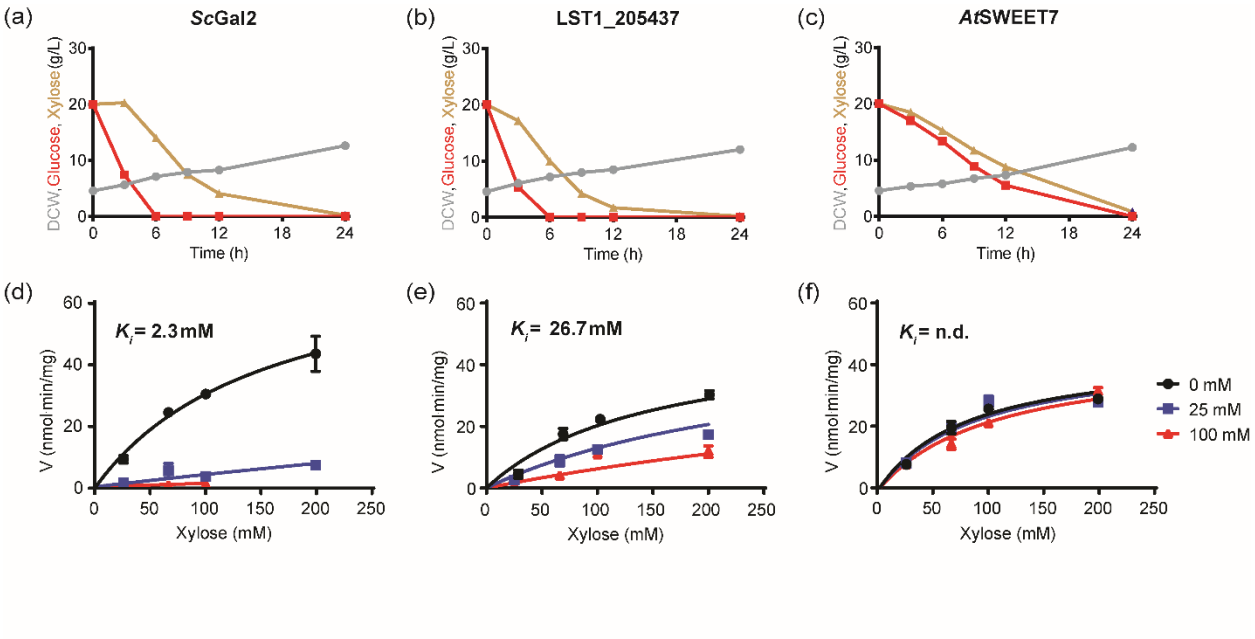

781

782 **Fig. 4: Glucose and xylose mixed sugar fermentation profile and inhibitory effect**
783 **of glucose on xylose transport.** 20 g/L of glucose and xylose mixed sugar fermentation
784 by SR8D8 expressing *Sc*Gal2 (sequential fermentation) (**a**), LST1_205437 (partial
785 cofermentation) (**b**), *At*SWEET7 (true co-fermentation) (**c**). Symbols: glucose (square),
786 xylose (triangle up), DCW (circle). Inhibitory effect of 0 mM, 25 mM and 100 mM glucose
787 on xylose transport in SR8D8 expressing *Sc*Gal2 (**d**), LST1_205437 (**e**) and *At*SWEET7
788 (**f**). Global curve fitting for Michaelis–Menten kinetics with competitive inhibition was
789 applied to data of three independent measurements at each concentration.
790

Fig. 5

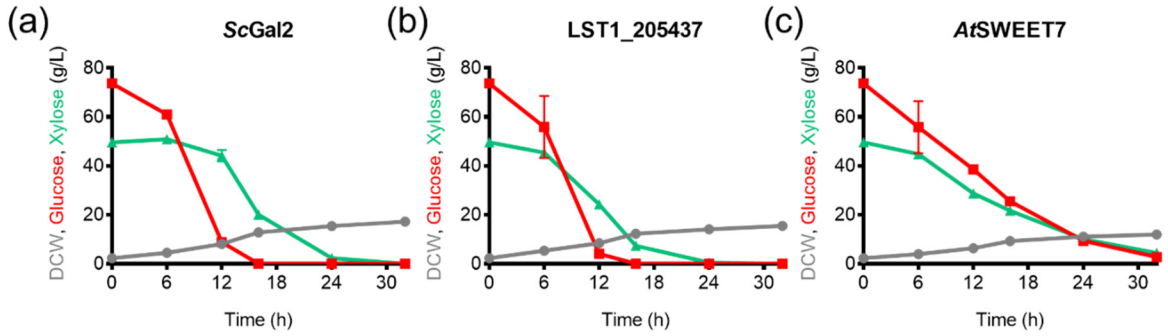

Fig. 5: Glucose and xylose mixed sugar fermentation profile using industrially relevant sugar concentrations. 70 g/L of glucose and 40g/L xylose mixed sugar fermentation by SR8D8 expressing *Sc*Gal2 (**a**), LST1_205437 (**b**), *At*SWEET7 (**c**). Symbols: glucose (square), xylose (triangle up), DCW (circle). The values are the means of two independent experiments, and the error bars indicate the standard errors

Fig. 6

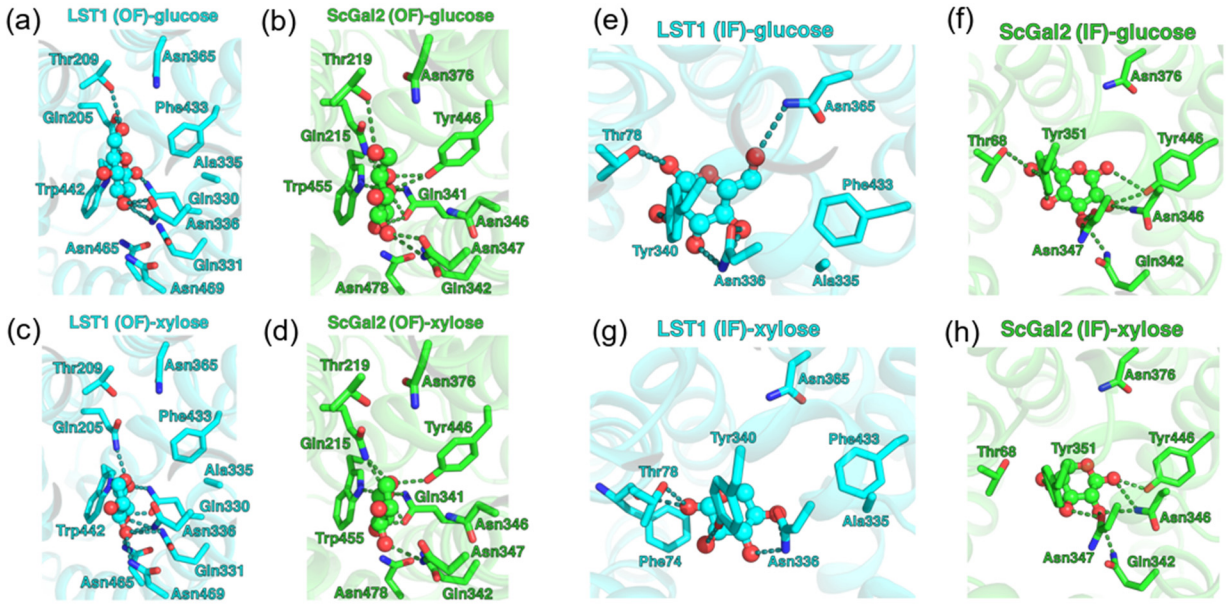

Fig. 6: Predicted binding orientation of glucose and xylose in *Sc*Gal2 and LST1_205437. The dock poses of glucose and xylose in OF conformations for LST1_205437 (**a, c**) and *Sc*Gal2 (**b, d**), respectively. The dock poses of glucose and xylose in IF conformations for LST1_205437 (**e, g**) and *Sc*Gal2 (**f, h**), respectively.

Fig. 7

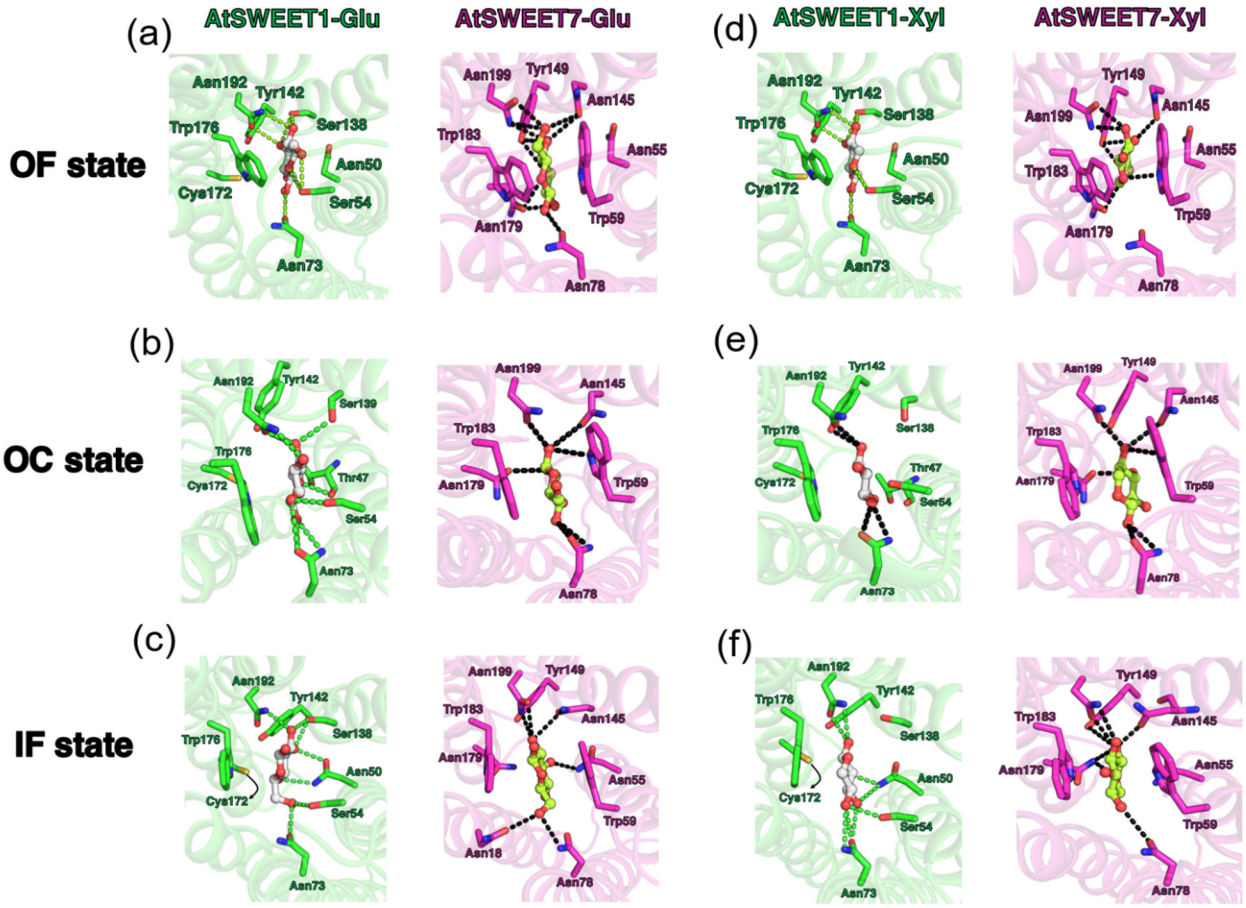

Fig. 7: Dockposes of glucose and xylose in *At*SWEET1 and *At*SWEET7. The predicted binding mode of glucose and xylose in *At*SWEET1 and *At*SWEET7 in OF (**a** and **d**), OC (**b** and **e**) and IF (**c** and **f**) conformations.

Fig. 8

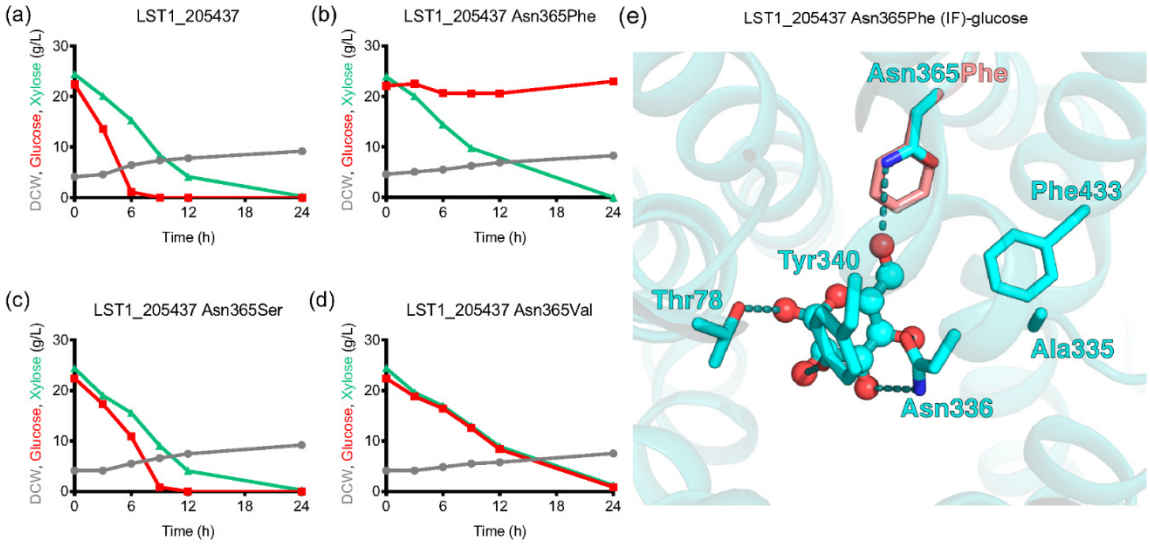

Fig. 8: Glucose and xylose mixed sugar fermentation profile of SR8D8 expressing LST1_205437 Asn365 mutant variants and glucose dockpose of LST1_205437 Asn365Phe. LST1_205437 Asn365Phe mutant, LST1_205437 Asn365Ser and LST1_205437 Asn365Val. 20 g/L of glucose and xylose mixed sugar fermentation in YP medium of LST1_205437 wild type (**a**), LST1_205437 Asn365Phe (**b**), LST1_205437 Asn365Ser (**c**) and LST1_205437 Asn365Val (**d**). Mutation of Asn365 to phenylalanine in LST1_205437 (**e**). Asn365 form crucial contact with glucose molecule in stabilize the IF state. The mutation to phenylalanine results in steric clash with substrate and affects the conformational transition to intermediate states and transport. Symbols: glucose (square), xylose (triangle up), DCW (circle). The values are the means of two independent experiments, and the error bars indicate the standard errors

Table 1 Kinetic properties of *Sc*Gal2, *At*SWEET7 and LST1_205437

Transporter	Glucose		Xylose		
	K_m (mM)	V_{max} (nmol·min^{-1}·mg^{-1})	K_m (mM)	V_{max} (nmol·min^{-1}·mg^{-1})	K_i (mM)
*Sc*Gal2	1.6 ± 0.2	38.3 ± 1.4	320.5 ± 70	88.7 ± 10.0	2.4 ± 0.5
*At*SWEET7	74.1 ± 13.0	110.3 ± 7.2	308.7 ± 86	100.9 ± 14.8	370.6 ± 109
LST1_205437	5.0 ± 1.0	47.0 ± 2.6	145.3 ± 43	76.8 ± 9.0	26.7 ± 6

Determined by zero-trans influx measurements with transporter-overexpressing SR8D8 and calculated with cell wet weight. SEM is indicated.